

Accelerated Publications

Measurements of Fluorescence Lifetimes by Use of a Hybrid Time-Correlated and Multifrequency Phase Fluorometer[†]

J. Hedstrom, S. Sedarous, and F. G. Prendergast*

Department of Biochemistry and Molecular Biology, Mayo Clinic/Foundation, Rochester, Minnesota 55905

Received May 17, 1988; Revised Manuscript Received June 28, 1988

ABSTRACT: Measurements of homogeneous and heterogeneous fluorescence intensity decays using a hybrid time-correlated single photon counting/multifrequency phase fluorometer are reported. A trio of fluorophores exhibiting a range of decay profiles was selected. *p*-Terphenyl, 1,4-bis[2-(4-methyl-5-phenyloxazolyl)]benzene [(Me)₂POPOP], and *p*-bis[2-(5-phenyloxazolyl)]benzene (POPOP), commonly used reference fluorophores, were analyzed initially; their emissions were characterized by monoexponential decay functions. Additionally, emissions from two single tryptophan proteins with different decay profiles were measured. Scorpion neurotoxin variant 3 required three exponentials to fit the emission decay properly (average lifetime ~500 ps). At pH 5.5, the fluorescence emission of ribonuclease T1 showed a monoexponential decay with a measured lifetime of ~4.0 ns. Thus, in each case, the results from both measurements were consistent between the two detection systems, confirming the view that the two approaches for measuring fluorescence lifetimes are equivalent.

The intrinsic sensitivity of fluorescence measurements, the time scale of excited-state fluorescence intensity decays (picoseconds to microseconds), and the sensitivity of fluorescence decay processes to environmental influences determine the importance of fluorescence lifetime measurements in studies of macromolecular structure and dynamics. Irrespective of whether the fluorescence derives from intrinsic fluorophores or from extrinsic fluorescence probes, the intensity decay data can reflect dynamic events occurring in the fluorophore's environment. The latter include solvent structure and dynamics, the dynamics of macromolecular conformation, quenching by exogenous agents, or ligand binding effects on macromolecules (Koester & Dowben, 1978; Lakowicz, 1983). Likewise, measurements of time-resolved fluorescence emission anisotropy, which afford quantitation of fluorophore motion (rates and amplitude), allow detection and quantitation of local fluorophore motion (Prendergast et al., 1981), of segmental or domain mobility, or of rotational rates of the entire macromolecule (Lakowicz, 1983).

There are two common techniques for measuring fluorescence lifetimes and anisotropy decays. The first method, time-correlated single photon counting (TCPC), requires that the fluorescent sample be stimulated by a δ -function excitation pulse of light and the time dependence of the emission detected (O'Connor & Phillips, 1984). In the second method, phase/modulation fluorometry, the sample is excited by an amplitude-modulated continuous wave (cw) light source, and the phase shift (and/or demodulation) of the emission is measured. In the latter method, the phase delay and the relative demodulation can be related simply to the fluorescence lifetime (Lakowicz, 1986). Early pulsed excitation schemes relied on flash lamps for excitation (Knight & Selinger, 1973). The broad, erratic pulse profiles from the lamps were a major limitation to the time resolution attainable from these in-

struments and to their accuracy, while the low repetition rates meant sometimes quite long data acquisition times. The main limitation in phase/modulation techniques has been the lack (until recently) of variable frequency modulation (Lakowicz, 1986). Early instruments were constrained to operate at only one to three fixed modulation frequencies; the consequent paucity of data points limited relatively easy and *reliable* analysis to monoexponential and biexponential decays.

Recent technological advances have resulted in substantially improved instrumentation and light sources for both TCPC and frequency domain fluorescence spectroscopy. Interestingly, the same advances that have significantly improved the performance of photon counting systems have proved equally beneficial for phase/modulation systems. In particular, the picosecond lasers now commonly used for TCPC measurements generate a train of temporally narrow, uniform pulses at a high repetition rate (Fleming, 1986; Shapiro, 1977). In the frequency domain, these pulses yield a large (quasi-continuous) series of equally spaced harmonic frequencies. This property of mode-locked lasers has been effectively exploited for the development of multifrequency phase fluorometers first by Gratton and co-workers (Alcala et al., 1985) and then subsequently by several other investigators, Lakowicz and colleagues being principal among the latter (Lakowicz, 1986). These new frequency domain fluorometers have shown clearly the power of multifrequency phase fluorometry (MPF), and yet the questions still exist implicitly and explicitly as to whether the two methods always yield the same results.

To date, however, comparisons of the relative performance of phase/modulation and TCPC systems have relied on information gathered from measurements done in different laboratories frequently with different experimental conditions even if the samples were the same protein or other macromolecules. Such data are clearly insufficient to allow for an accurate assessment of the relative merits of the two methods or even to answer the simple question as to whether both methods would yield the same value for fluorescence intensity decays. We report here on measurements of fluorescence lifetimes made on a hybrid TCPC/MPF instrument. This

[†] The development of the TCPC component of the hybrid fluorometer was supported by Grant RR04218, and the work overall was supported by Grant GM34847 from the USPHS. J.H. was supported by NIH Training Grant DK07198.

* Author to whom correspondence should be addressed.

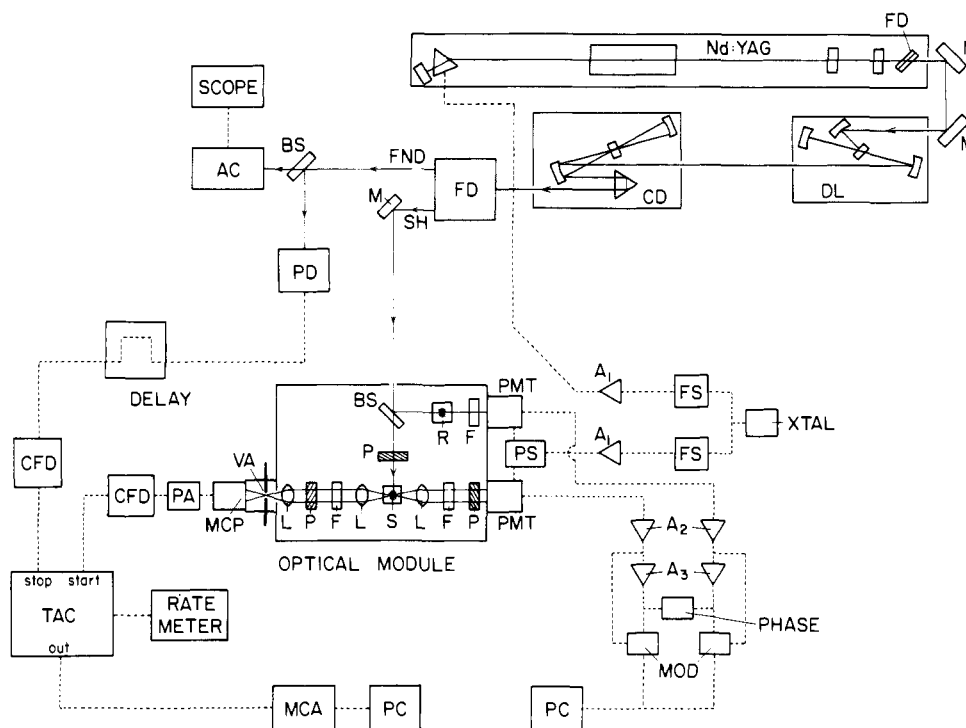


FIGURE 1: Schematic of hybrid time-correlated single photon counting/multifrequency phase-modulation fluorometer: L, lens; F, filter; VA, variable aperture; PMT, photomultiplier tube; MCP, microchannel plate; PS, power splitter; A₁, rf amplifier; A₂, DC amplifier; A₃, AC tuned amplifier; FS, frequency synthesizer; XTAL, 10-MHz quartz oscillator; PA, preamplifier; CFD, constant fraction discriminator; FD, frequency doubler; M, mirror; DL, dye laser; CD, cavity dumper; FND, dye laser fundamental; SH, dye laser second harmonic; BS, beam splitter; AC, real-time autocorrelator; PD, photodiode; P, polarizer; S, sample.

instrument utilizes a single synchronously pumped and mode-locked Nd:YAG laser as an excitation source for simultaneous photon counting and phase fluorometric examination of a single fluorescent sample. The results show that both methods yield consistent data for samples that exhibit either single or (apparently) multiexponential fluorescence intensity decays.

MATERIALS AND METHODS

Laser and Optical Design. The 1064-nm fundamental from a Spectra Physics (SP) Model 3400 Nd:YAG laser was acoustooptically mode-locked by an SP 342A mode-locker head driven at 41.072318 MHz. The frequency synthesis was provided by a Hewlett-Packard (HP) 3335A synthesizer (200 Hz–80 MHz, 0.001-Hz resolution). The laser output was frequency-doubled (SP 3220-1 frequency doubler, angle-tuned KTP crystal) and used to synchronously pump a rhodamine 6G dye laser (SP 375B-91, tunable with a three-plate Lyot filter between 570 and 640 nm). The pulse repetition rate of the dye laser was controlled by an SP 344 cavity dumper. Output pulses were up-converted with an SP 390 frequency doubler employing an angle-tuned KDP crystal. The lasing wavelength of the dye laser was tuned to 590 nm and the cavity-dumper repetition rate set at 4 MHz for all reported work. Cavity-dumper output pulse widths (~10 ps FWHM) were monitored continuously by passing the fundamental output from the SP 390 frequency doubler into an Inrad Model 5-14 real-time autocorrelator. The average powers of the dye laser fundamental and second harmonic were ~300 and 4 mW, respectively. The 295-nm pump pulse beam waist was ~1 mm in diameter. Incident laser intensities were attenuated by greater than an order of magnitude with neutral density filters.

The UV pulses, initially horizontally polarized, were rotated to the magic angle (Special Optics polarization rotator, fol-

lowed by an SLM "cleanup" polarizer) before passing into the SLM sample chamber. An ~5% fraction of the beam was split off to excite a reference solution (for MPF measurements) of ~10⁻⁶ M *p*-terphenyl dissolved in cyclohexane. The remaining beam was used to excite the sample.

Fluorescence Detection. The two detection systems (for photon counting and multifrequency fluorometry) were laid out in a t-format (Figure 1) of an SLM optical module. For the MPF system a 7-cm focal length (f₁) fused silica lens was used to collimate the fluorescence and direct it to a Hamamatsu R928 photomultiplier tube (PMT). A 10-nm band-pass (bp) interference filter centered on 320 nm and blocked to infinity passed the fluorescence while blocking the scattered light from the detector.

Cross-correlation detection was accomplished by applying a small radio-frequency (rf) signal to the second dynode of the PMTs. The source of the modulation was an HP 8662A synthesized signal generator (10 kHz–1280 MHz, 0.1-Hz resolution) whose 10-mV output was amplified (ENI Model 603L rf power amplifier; 40-dB gain from 0.8 to 1000 MHz) prior to the PMT dynodes. The modulation frequency was selected to be offset by 25 Hz (cross-correlation frequency) from the desired Fourier component of the exciting laser pulse. The modulated signals from the reference and sample PMTs were input to an ISS spectrofluorometer for subsequent phase and modulation analysis. The output files were transferred to an IBM PC computer for data analysis.

Fluorescence for TCPC was collected into a second PMT mounted on the second side of the t-format and collimated with a 4-cm f₁ fused silica lens. A second 7-cm f₁ fused silica lens focused the emission through a variable rectangular aperture onto a Hamamatsu 1564U-03 microchannel plate (MCP). The MCP exhibited ~6 × 10⁵ gain and 78-ps transit time spread at 3000 V, 500 nm. The same interference filters used for MPF detection were used in TCPC applications. MCP

Table I: Discrete Component Analysis of TCPC and MPF Data

	τ_1 (ns)	f_1	τ_2 (ns)	f_2	τ_3 (ns)	f_3	χ_r^2
<i>p</i> -terphenyl in cyclohexane							
TCPC ^a	0.947 ± 0.004	1.00					1.06
(Me) ₂ POPOP in EtOH							
TCPC	1.413 ± 0.006	1.00					1.43
POPOP in EtOH							
TCPC	1.315 ± 0.013	1.00					1.26
MPF ^b	1.304 ± 0.003	1.00					1.60
SN3 in buffer (pH 7.0)							
TCPC	2.36	0.06	0.510	0.72	0.173	0.22	1.26
MPF	2.631 ± 0.464	0.102 ± 0.019	0.474 ± 0.035	0.777 ± 0.036	0.022 ± 0.072	0.121 ± 0.020	1.52
RNase T1 in buffer (pH 5.5)							
TCPC	3.890 ± 0.020	1.00					2.17
	3.920 ± 0.017	0.997	0.110 ± 0.022	0.003			1.26
MPF	4.087 ± 0.011	1.00					1.88
	4.123 ± 0.008	0.997	-0.166 ± 0.492	0.003			0.613

^aTCPC data collected at 10 ps/channel resolution, except SN3 data (20 ps/channel). ^bMPF data collected with $\sigma_p \leq 0.2$ and $\sigma_m \leq 0.005$, except SN3 ($\sigma_p \leq 0.6$; $\sigma_m \leq 0.004$).

photocurrent pulses were amplified by a B&H Electronics AC3011 LN (1.4-GHz) 24-dB preamplifier. Amplified pulses were passed through one channel (modified by Tennelec for MCP use; 0.5 fraction) of a Tennelec TC455 quad constant fraction discriminator and served as start pulses (inverted configuration) in an Ortec 566 time-to-amplitude convertor (TAC). An EG&G FOD-100 photodiode, operating in the photoconduction mode, was used to sample the dye laser fundamental output. Its signal was processed through an unmodified channel (0.2 fraction) of the CFD to provide stop pulses. The TAC output was passed through an Ortec 408A biased amplifier and stored in an Ortec Ace-2K multichannel analyzer (MCA) plug-in card housed in an AST personal computer (IBM AT compatible). The biased amplifier was adjusted to yield either 10.0- or 20.0-ps channel resolution in the MCA with an Ortec Model 462 time calibrator.

Instrument response functions (~ 90 ps FWHM) for deconvolution of raw data were obtained by collecting the scattering at 295 nm (291.5 nm, 5-nm bp interference filter) from a sample of nondairy creamer in distilled water. The same experimental sample was used for both TCPC and MPF measurements.

Materials. Samples were chosen to permit comparisons between detection systems over a range of fluorophore lifetimes. *p*-Terphenyl was purchased from Eastman Kodak; *p*-bis[2-(5-phenyloxazolyl)]benzene (POPOP) and 1,4-bis[2-(4-methyl-5-phenyloxazolyl)]benzene [(Me)₂POPOP] were from New England Nuclear. The protein samples, ribonuclease T1 (RNase T1) and scorpion neurotoxin variant 3 (SN3), were the kind gifts of Dr. Fred Walz, Kent State University, and Dr. Dean Watt, Creighton University, respectively. *p*-Terphenyl concentration was adjusted to 1 μ M in cyclohexane (HPLC grade from Fisher Scientific). POPOP and (Me)₂POPOP concentrations were 10 μ M in absolute ethanol. RNase T1 was prepared in a buffer solution containing 1 mM (reagent grade) sodium acetate (pH 5.5) and 0.3 M KCl to yield a final protein concentration of 7 μ M. SN3 concentration was adjusted to 15 μ M in 0.25 mM MOPS buffer (pH 7.0) containing 0.125 M KCl. Solution temperatures were maintained at 25 °C with a Brinkmann RC3 external bath circulator connected to the sample holder.

RESULTS AND DISCUSSION

Both *p*-terphenyl and (Me)₂POPOP were used as reference fluorophores for MPF measurements which were made with 340-nm (10-nm band-pass) and 450-nm (5-nm band-pass) interference filters used in the collection optics, respectively. A lifetime of 0.99 ns was assigned for *p*-terphenyl in cyclo-

hexane, on the basis of previous measurements using MPF (Gratton et al., 1984; Alcala et al., 1987). The *p*-terphenyl lifetime was also measured independently with our photon counting system. The resulting lifetime (0.950 ± 0.005 ns) was similar to that obtained from the MPF measurements. Monoexponential fits to the TCPC decay profiles of *p*-terphenyl yielded reduced χ_r^2 of ~ 1.05 . Similarly, the reference lifetime for (Me)₂POPOP was measured by using TCPC. The resulting 1.41 ± 0.005 ns lifetime correlates well with published data (Lakowicz, 1983) and was used as the reference value for (Me)₂POPOP in subsequent MPF measurements.

The first measurements employing both TCPC and MPF were made on POPOP. (Me)₂POPOP was the reference fluorophore for MPF measurements. As can be seen in Table I, there is excellent agreement between the measured lifetimes. Additionally, both sets of data coincide with literature values of τ for POPOP in ethanol (Lakowicz, 1983).

SN3 provided an interesting test for the two systems. Not only is the average lifetime extremely short (~ 500 ps) but also the fluorescence decay is clearly not monoexponential. While we are not attempting here to attach any physical significance to each lifetime component, the degree of correlation between the individual lifetime constituents would provide a meaningful comparison between the two detection systems. The time-resolved emission from SN3 was well fit by a triexponential model decay function ($\chi_r^2 = 1.22$), with an average lifetime of 0.55 ns (see Figure 2). Again, the MPF results correlated excellently with the TCPC findings. A triexponential fit to the data yielded a χ_r^2 of 1.52 and a lifetime average of 0.50 ns (see Figure 3). Table I shows the recovered values for both data sets.

The choice of a triexponential model function for the SN3 fluorescence decay is purely phenomenological in the sense that, for a single tryptophan protein, it suggests the existence of three distinct protein conformations. Clearly, this inference is biased by the use of a discrete exponential decay model. We have grown accustomed to interpreting fluorescence intensity decay curves in terms of exponential models, from which one or more fluorescence lifetime components are assigned on the basis of an appropriate statistical fitting procedure. However, the limited resolvability of the data in lifetime components provided by current instrumentation (either TCPC or MPF) does not allow one to distinguish among the different factors involved in the decay process. It is, therefore, not surprising that some variation between the recovered amplitude and lifetime components is seen between data sets for SN3. The recovered values may reflect the time resolution of each method or the fact that a discrete exponential decay model

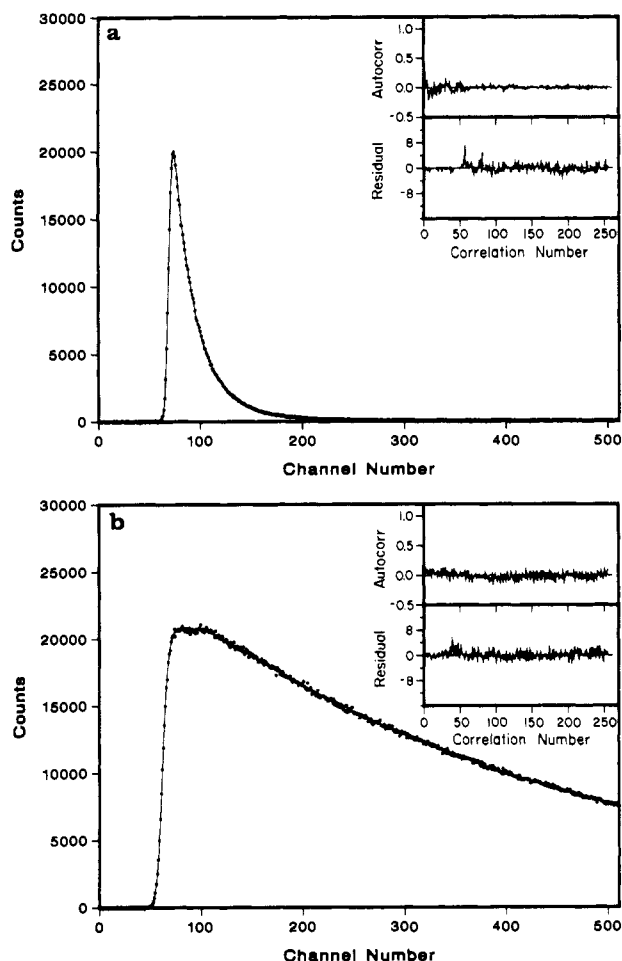


FIGURE 2: Time-domain fluorescence profiles of (a) SN3 in MOPS buffer (pH 7.0) and (b) RNase T1 in sodium acetate buffer (pH 5.5). Continuous curves are optimized convolutions [Marquardt algorithm (Marquardt, 1963)] of triexponential (SN3) and biexponential (RNase T1) decay functions with the impulse response function. Lower and upper inset plots show the residuals and autocorrelations of the residuals, respectively, for each sample.

is not appropriate. The observed signal may easily constitute a superposition of heterogeneous decays comprising individual lifetime values that are very close to one another; i.e., a distribution model might be a better description of the physical situation as has been suggested (Alcala et al., 1987).

Multieponential decay is the rule rather than the exception in many proteins containing a single tryptophan residue (Beechem & Brand, 1985). RNase T1 in aqueous buffer is interesting in this regard, since its fluorescence decay is biexponential *except* at low pH, where the decay is reportedly monoexponential. RNase T1 lifetimes have been measured in different laboratories (Chen et al., 1987; Eftink & Ghiron, 1987) by using photon counting and phase/modulation detection, respectively. Fleming and co-workers (Chen et al., 1987) reported that, at pH 5.5 and 20 °C, RNase T1 decays monoexponentially with a lifetime of 4.04 ns ($\chi_r^2 = 1.12$). Eftink and Ghiron (1987), fitting their data to a single exponential model, reported a shorter lifetime ($\tau = 3.65$ ns) with a large χ_r^2 . Fitting their data to a biexponential decay reduced the χ_r^2 by greater than a factor of 3, but the authors did not feel that this was a sufficient improvement in the χ_r^2 to give credence to the τ values found with the two-component fit. Since there is some disparity between these reported lifetimes for RNase T1, we have repeated these measurements on our dual detection instrument. A single-component fit to both our TCPC and MPF data recovers a 3.92- and 4.08-ns lifetime,

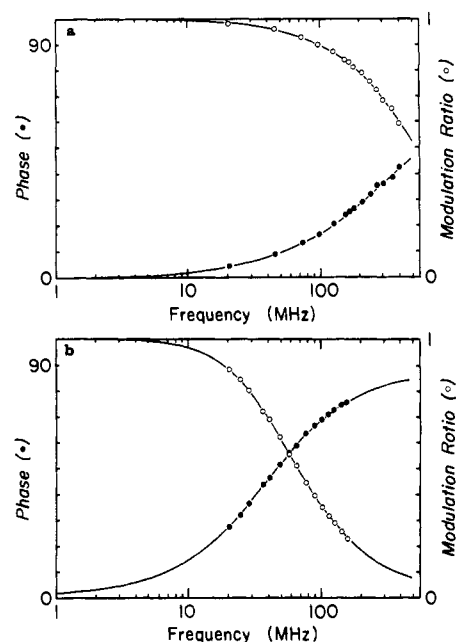


FIGURE 3: Multifrequency phase/modulation data for (a) SN3 in MOPS buffer (pH 7.0) and (b) RNase T1 in sodium acetate buffer (pH 5.5). The solid lines are the best tri- and biexponential fits to the SN3 and RNase T1 data, respectively.

respectively, for RNase T1 (cf. 4.04 ns from Fleming's group). We also note that by including a second component with a short lifetime we improve the fit to our data, although it does not significantly alter the value of the main component. In TCPC, this corresponded to a mere 0.3% fraction, 100-ps lifetime component. We recovered a similar fractional contribution from the multifrequency phase fluorometric data for a component with an apparent lifetime of ~ 166 ps. However, the uncertainty in this latter lifetime was ± 492 ps. In an attempt to ferret out the origin of this component, a control experiment was run on the TCPC system with just a sample of the buffered solvent in the cuvette. A very low intensity, short-lived signal was detected under these conditions, which suggested that the short component detected in the RNase T1 decays might be due to the transmission of scattered light through the interference filter. Measurements of fluorescence spectra of the buffered solvent failed to show any fluorescent contaminant. Chen et al. (1987) had used a monochromator/cutoff filter (Schott WG335) combination to eliminate scattered light and minimize filter fluorescence. Eftink and Ghiron (1987) had observed the RNase T1 emission through a Corning 7-60 cutoff filter. On the basis of our results, it seems possible that the small second component observed by Eftink was due to transmitted scatter and/or filter fluorescence. The main component (90%) of their biexponential fit to the RNase T1 decay yielded a lifetime of 4.07 ns, essentially identical with what Chen et al. (1987) had found and with the value we now report.

On the basis of the results we have presented here, it is clear that TCPC and MPF techniques are capable of measuring both rapid and multieponential fluorescence intensity decays. It should be noted, however, that the resolvability of either technique is ultimately limited by the uncertainty associated with the individual data points. For example, increasing the variance in the number of counts/channel (by reducing the integrated counts in the decay profile) leads to poorer resolvability in TCPC. Similarly, if the standard deviations for individual phase and/or modulation measurements are raised, this will limit the resolvability of the MPF technique. Further

comparisons between TCPC and MPF should involve measurement of even shorter decays and in particular a comparison of time-dependent anisotropy of very fast (picosecond time scale) fluorophore motion. In this limit, we would expect the MPF measurements to be limited by the modulation and frequency response of the photomultiplier tube.

Finally, it is worthwhile to consider the relative merits of TCPC and MPF techniques, which is a constant question in many investigators' minds. With the data presented here we can safely assume that the accuracy issue is settled and what we need now to do is to consider from the strictly instrumental standpoint the merits of each approach.

Apart from the improvement in TCPC measurements which came with the advent of picosecond lasers, advances in photomultiplier tube technology have also played a key role in extending the applicability of these systems. Impulse response functions of less than 100 ps (FWHM) can be obtained routinely by use of picosecond laser excitation with microchannel plate photomultiplier tubes as light detectors (Hamamatsu, 1987). As a corollary, substitution of an MCP for a conventional PMT in frequency-domain fluorometers has extended the upper modulation frequency limit from ~ 500 MHz to at least 2 GHz (Lakowicz et al., 1986). However, there are other features of TCPC that make the method valuable for quantifying fluorescence intensity decays (O'Connor & Phillips, 1984; Lakowicz, 1986). Thus, because TCPC is a "digital" form of light detection relying on the detection of individual photons, excitation intensity and optical efficiency are less important than in analog detection methods. Further, the photon counting approach offers excellent low light level sensitivity, can yield a wide dynamic range of data, and is relatively insensitive to drift in photodetector supply voltage, excitation intensity variation, or temperature fluctuations. Additionally, TCPC is intuitively direct and the data exhibit counting statistics that obey a Poisson distribution (Bevington, 1969), which means that, in data workup, the statistical information required for properly weighting each point is known. Conversely, for MPF there remains a question regarding the accepted method for weighting the data. Typically, data are collected until the standard deviations from each set of measurements of phase and modulation lie below a preset upper limit (common for all modulation frequencies). These limiting standard deviations are used subsequently in data analysis, and the true deviations are therefore often overestimated. The time resolution achieved in TCPC is not limited to the PMT anode pulse width, but is in principle limited only by the statistical dispersion in the PMT pulse transit times (transit time spread) (O'Connor & Phillips, 1984). Lastly, TCPC lends itself to a convolute-and-compare least-squares analysis (Grinvald & Steinberg, 1974), allowing decay times shorter than the instrument response FWHM to be accurately measured. The shortest lifetime that can be recovered by using the convolute-and-compare analysis is estimated to be $1/15$ of the instrument response FWHM for a single exponential decay (O'Connor & Phillips, 1984). Interestingly, one of the initial apparent disadvantages of the TCPC method was the relatively long acquisition time for data collection compared to a typical three-frequency phase measurement. With currently available technology MPF measurements now take considerably longer than a typical TCPC acquisition when laser excitation is employed for the latter.

Multifrequency phase fluorometry also has several features which recommend the method. For example, the cross-correlation methods used for signal detection allow for measurements of phase delays and relative demodulation ratios

with high sensitivity, low noise, and consequently good accuracy. The limiting light level for multifrequency fluorometers is in the range of 100–1000 photons/s (Gratton et al., 1984)—roughly comparable to the lower range found for TCPC measurements. Seemingly, MPF has an advantage over TCPC in that since phase delays and modulation ratios are measured relative to the incident radiation, there is no need to deconvolute the instrument function from the accumulated data. However, this advantage of not requiring deconvolution is only apparent since the convolution is "removed" by treating the emission and excitation wave forms as a ratio. This procedure assumes that any systematic errors will cancel exactly—an assumption which may not always be valid. Frequency domain methods are also uniquely suited to the measurement of rapid decays of fluorescence anisotropy, because the signal corresponding to rotational diffusion can be measured directly (Gratton et al., 1984). Rotational correlation times down to 15 ps have been claimed from 2-GHz frequency domain measurements (Lakowicz et al., 1986), and it therefore seems that at the moment MPF employing a microchannel plate PMT as detector would be the technique of choice for measurement of rotational motions occurring in the low picosecond time frame. At least one instrument manufacturer, Hamamatsu, has constructed a MCP-PMT designed especially for use with MPF.

In summary, it is clear that both the MPF and TCPC techniques are capable of providing consistent and accurate information of fluorescence intensity decays. The principal effort should now be directed toward the interpretation of the data; in particular, more effort should be expended on further evaluation of recent suggestions that heterogeneous fluorescence intensity decays (especially in macromolecules bearing single fluorophores) should be interpreted in terms of distributions rather than as multiple exponential forms (Alcala et al., 1985; James & Ware, 1985; Livesey & Brochon, 1987). Simultaneous measurement of lifetimes by both MPF and TCPC affords the ideal situation not only because the results should be corroborated but also, and especially, for providing the optimal opportunity to apply global analysis procedures.

ACKNOWLEDGMENTS

We thank Dr. E. Gratton, whose help was invaluable in developing MPF techniques in our laboratory, Dr. Walter Struve for having shared his data analysis software with us, and the reviewers for their helpful comments. We also thank Peter Callahan for his help in preparing the figures and Linda Wilkin and Pat Hart for typing.

REFERENCES

- Alcala, J. R., Gratton, E., & Jameson, D. M. (1985) *Anal. Instrum.* 14, 225–250.
- Alcala, J. R., Gratton, E., & Prendergast, F. G. (1987) *Biophys. J.* 51, 925–936.
- Beechem, J. M., & Brand, L. (1985) *Annu. Rev. Biochem.* 54, 4371.
- Bevington, P. R. (1969) in *Data Reduction and Error Analysis for the Physical Sciences*, pp 36–43, McGraw-Hill, New York.
- Chen, L. X.-Q., Longworth, J. W., & Fleming, G. R. (1987) *Biophys. J.* 51, 865–873.
- Eftink, M. R., & Ghiron, C. A. (1987) *Biophys. J.* 52, 467–473.
- Fleming G. R. (1986) in *Chemical Applications of Ultrafast Spectroscopy*, pp 91–96, Oxford University Press, New York.

- Gratton, E., Jameson, D. M., & Hall, R. D. (1984) *Annu. Rev. Biophys. Bioeng.* 13, 105-124.
- Grinvald, A., & Steinberg, I. Z. (1974) *Anal. Biochem.* 59, 583-598.
- Hamamatsu Technical Memorandum ET-03 (1987) Hamamatsu Corp., Bridgewater, NJ.
- James, D. R., & Ware, W. R. (1985) *J. Phys. Chem.* 89, 5450-5458.
- Knight, A. E. W., & Selinger, B. K. (1973) *Aust. J. Chem.* 26, 1-27.
- Koester, V. J., & Dowben, R. M. (1978) *Rev. Sci. Instrum.* 49, 1186-1191.
- Lakowicz, J. R. (1983) *Principles of Fluorescence Spectroscopy*, pp 316-331, Plenum, New York.
- Lakowicz, J. R. (1986) *Applications of Fluorescence in the Biomedical Sciences*, pp 225-244, Alan R. Liss, New York.
- Lakowicz, J. R., Laczko, G., & Gryczynski, I. (1986) *Rev. Sci. Instrum.* 57, 2499-2506.
- Livesey, A. K., & Brochon, J. C. (1987) *Biophys. J.* 52, 693-706.
- Marquardt, D. W. (1963) *J. Soc. Ind. Appl. Math.* 11, 431-441.
- O'Connor, D. V., & Phillips, D. (1984) in *Time-Correlated Single Photon Counting*, pp 36-52, Academic, Orlando.
- Prendergast, F. G., Haugland, R. P., & Callahan, P. J. (1981) *Biochemistry* 20, 7333-7338.
- Shapiro, S. L. (1977) in *Ultrashort Light Pulses*, pp 18-23, Springer-Verlag, New York.

Articles

Properties of the Binding Sites for the *sn*-1 and *sn*-2 Acyl Chains on the Phosphatidylinositol Transfer Protein from Bovine Brain[†]

P. A. van Paridon,^{*,‡} T. W. J. Gadella, Jr.,[‡] P. J. Somerharju,[§] and K. W. A. Wirtz[†]

Laboratory of Biochemistry, State University of Utrecht, Transitorium III, Padualaan 8, NL-3584 CH Utrecht, The Netherlands, and Department of Basic Chemistry, University of Helsinki, Siltavuorenpenger 10, 00170 Helsinki 17, Finland

Received December 16, 1987

ABSTRACT: We have studied the properties of the fatty acyl binding sites of the phosphatidylinositol transfer protein (PI-TP) from bovine brain, by measuring the binding and transfer of pyrenylacyl-containing phosphatidylinositol (PyrPI) species and pyrenylacyl-containing phosphatidylcholine (PyrPC) species as a function of the acyl chain length. The PyrPI species carried a pyrene-labeled acyl chain of variable length in the *sn*-2 position and either palmitic acid [C(16)], palmitoleic acid [C(16:1)], or stearic acid [C(18)] in the *sn*-1 position. Binding and transfer of the PI species increased in the order C(18) < C(16) < C(16:1), with a distinct preference for those species that carry a pyrenyloctanoyl [Pyr(8)] or a pyrenyldecanoyl [Pyr(10)] chain. The PyrPC species studied consisted of two sets of positional isomers: one set contained a pyrenylacyl chain of variable length and a C(16) chain, and the other set contained an unlabeled chain of variable length and a Pyr(10) chain. The binding and transfer experiments showed that PI-TP discriminates between positional isomers with a preference for the species with a pyrenylacyl chain in the *sn*-1 position. This discrimination is interpreted to indicate that separate binding sites exist for the *sn*-1 and *sn*-2 acyl chains. From the binding and transfer profiles it is apparent that the binding sites differ in their preference for a particular acyl chain length. The binding and transfer vs chain length profiles were quite similar for C(16)Pyr(x)PC and C(16)Pyr(x)PI species, suggesting that the *sn*-2 acyl chains of PI and PC share a common binding site in PI-TP.

Phospholipid transfer proteins belong to a group of soluble cytosolic proteins which presumably take part in the transport of phospholipids between the intracellular membranes (Wirtz, 1982). These proteins are able to discriminate between phospholipid classes and species (Wirtz, 1982; Kader et al., 1983; Zilversmit, 1984). It has been proposed that this property is essential for the maintenance of the phospholipid composition of the intracellular membranes (Kaplan & Simoni, 1985).

In view of the important physiological function of phosphoinositides, it is of considerable interest that in all mammalian cells investigated to date a protein has been detected

that binds and transfers phosphatidylinositol (PI)¹ between membranes (Helmkamp et al., 1974; DiCorleto et al., 1979; Daum & Paltauf, 1984; George & Helmkamp, 1985). The PI transfer protein from bovine brain (PI-TP) has been studied in considerable detail [for reviews, see Wirtz (1982) and Helmkamp (1985)]. This protein preferentially transfers PI but can also transfer phosphatidylcholine (PC) (DiCorleto et

¹ Abbreviations: C(16:1), palmitoleic acid; C(20:4), arachidonate; PI, phosphatidylinositol; PC, phosphatidylcholine; PA, phosphatidic acid; PyrPI, pyrenylacyl-containing phosphatidylinositol (see Figure 1 for the nomenclature of the PyrPI species); PyrPC, pyrenylacyl-containing phosphatidylcholine (see Figure 1 for the nomenclature of the PyrPC species); TNP-PE, *N*-(trinitrophenyl)phosphatidylethanolamine; PI-TP, phosphatidylinositol transfer protein; PC-TP, phosphatidylcholine transfer protein; DMSO, dimethyl sulfoxide; Tris, tris(hydroxymethyl)aminomethane; EDTA ethylenediaminetetraacetic acid; HPLC, high-performance liquid chromatography.

[†] This research was supported by grants from the Finnish Academy, the European Molecular Biology Organization (EMBO), and the Federation of Biological Sciences (FEBS) to P.J.S.

[‡] State University of Utrecht.

[§] University of Helsinki.